Fast light in silicon ring resonator with resonance-splitting

Qiang Li,[1] Ziyang Zhang,[2] Jing Wang,[2] Min Qiu,[2] and Yikai Su[1,*]

[1]State Key Lab of Advanced Optical Communication Systems and Networks, Department of Electronic Engineering, Shanghai Jiao Tong University, 800 Dongchuan Rd, Shanghai 200240, China
[2] Department of Microelectronics and Applied Physics, Royal Institute of Technology, Electrum 229, 164 40 Kista, Sweden
[*]Corresponding author: yikaisu@sjtu.edu.cn

Abstract: We report experimental demonstration of fast light in an over-coupled ultra-compact silicon ring resonator with resonance-splitting. Strong mutual-coupling induced by the grating inside the ring leads to split resonances and accompanying large anomalous dispersion, thus providing a new approach to realizing fast light in the over-coupled region of the ring resonator. In the experiment, a maximum pulse advancement of 130 ps with low distortion is achieved for a 1-ns signal pulse in a 10-μm-radius silicon ring resonator. The observed pulse advancement agrees well with the theoretical calculation based on coupled mode theory.

OCIS codes: (130.3120) Integrated optics devices; (230.4555) Coupled resonators;

References and links

1. R. W. Boyd, D. J. Gauthier, and A. L. Gaeta, "Applications of slow-light in telecommunications," Opt. Photonics News **17**, 18-23 (2006).
2. E. Parra and J. R. Lowell, "Toward applications of slow light technology," Opt. Photonics News **18**, 40-45 (2007).
3. L. J. Wang, A. Kuzmich, and A. Dogariu, "Gain-assisted superluminal light propagation," Nature **406**, 277-279 (2000).
4. A. Kuzmich, A. Dogariu, L. J. Wang, P. W. Milonni, and R. Y. Chiao, "Signal velocity, causality, and quantum noise in superluminal light pulse propagation," Phys. Rev. Lett. **86**, 3925-3929 (2001).
5. M. D. Stenner, D. J. Gauthier, and M. A. Neifeld, "The speed of information in a 'fast-light' optical medium," Nature **425**, 695-698 (2003).
6. R. Y. Chiao and P. W. Milonni, "Fast Light, Slow Light," Opt. Photonics News **13**, 26-30 (2002),.
7. K. Y. Song, M. González Herráez, and L. Thévenaz, "Gain-assisted pulse advancement using single and double Brillouin gain peaks in optical fibers," Opt. Express **13**, 9758-9765 (2005).
8. A. Schweinsberg, N. N. Lepeshkin, M. S. Bigelow, R. W. Boyd, and S. Jarabo, "Observation of superluminal and slow light propagation in erbium-doped optical fiber," Europhys. Lett. **73**, 218-224 (2006).
9. G. M. Gehring, A. Schweinsberg, C. Barsi, N. Kostinski, and R. W. Boyd, "Observation of backward pulse propagation through a medium with a negative group velocity," Science **312**, 895-897 (2006).
10. H. Shin, A. Schweinsberg, G. Gehring, K. Schwertz, H. J. Chang, R. W. Boyd, Q. Park, and D. J. Gauthier, "Reducing pulse distortion in fast-light pulse propagation through an erbium-doped fiber amplifier," Opt. Lett. **32**, 906-908 (2007).
11. M. S. Bigelow, N. N. Lepeshkin, and R. W. Boyd, "Superluminal and slow-light propagation in a room-temperature solid," Science **301**, 200-202 (2003).
12. H. Su and S. L. Chuang, "Room temperature slow and fast light in a quantum-dot semiconductor amplifier," Appl. Phys. Lett. **88**, 061102 (2006).
13. B. Pesala, F. Sedgwick, A. V. Uskov, and C. Chang-Hasnain, "Electrically tunable fast light at THz bandwidth using cascaded semiconductor optical amplifiers," Opt. Express **15**, 15863-15867 (2007).
14. B. Pesala, Z. Chen, A. V. Uskov, and C. Chang-Hasnain, "Experimental demonstration of slow and superluminal light in semiconductor optical amplifiers," Opt. Express **14**, 12968-12975 (2006).
15. L. J. Wang, A. Kuzmich, and A. Dogariu, "Gain-assisted superluminal light propagation," Nature **406**, 277-279 (2000).
16. Md. A. I. Talukder, Y. Amagishi, and M. Tomita, "Superluminal to subluminal transition in the pulse propagation in a resonant absorbing medium," Phys. Rev. Lett. **86**, 3546-3549 (2001).
17. G. Dolling, C. Enkrich, M. Wegener, C. M. Soukoulis, and S. Linden, "Simultaneous negative phase and group velocity of light in a metamaterial," Science **312**, 892-894 (2006).

18. K. Totsuka and M. Tomita, "Slow and fast light in a microsphere-optical fiber system," J. Opt. Soc. Am. B **23**, 2194-2199 (2006).
19. K. Totsuka and M. Tomita, "Observation of fast light in Mie scattering processes," Phys. Rev. E **73**, 045602(R) (2006).
20. G. T. Reed, "The optical age of silicon," Nature **427**, 595-596 (2004).
21. B. Jalali, "Teaching silicon new tricks," Nat. Photonics **1**, 193-195 (2007).
22. F. N. Xia, L. Sekaric, and Y. Vlasov, "Ultracompact optical buffers on a silicon chip," Nat. Photonics **1**, 65-71 (2007).
23. J. Scheuer, G. T. Paloczi, J. Poon, and A. Yariv, "Coupled resonator optical waveguides: toward the slowing and storage of light," Opt. Photonics News, **16**, 36-40 (2005).
24. J. E. Heebner and R. W. Boyd, "'Slow' and 'fast' light in resonator-coupled waveguides," J. Mod. Opt. **49**, 2629-2636 (2002).
25. Z. Zhang, M. Dainese, L. Wosinski, and M. Qiu, "Resonance-splitting and enhanced notch depth in SOI ring resonators with mutual mode coupling," Opt. Express **16**, 4621-4630 (2008).
26. B. E. Little, S. T. Chu, H. A. Haus, J. Foresi, and J. P. Laine, "Microring resonator channel dropping filters," IEEE J. Lightwave Technol. **15**, 998-1005 (1997).
27. C. Manolatou, M. J. Khan, S. Fan, P. R. Villeneuve, H. A. Haus, and J. D. Joannopoulos, "Coupling of modes analysis of resonant channel add-drop filters," IEEE J. Quantum Electron. **35**, 1322-1331 (1999).
28. D. D. Smith and H. Chang, "Coherence phenomena in coupled optical resonators," J. Mod. Opt. **51**, 2503-2513 (2004).
29. S. Scheerlinck, J. Schrauwen, F. Van Laere, D. Taillaert, D. Van Thourhout, and R. Baets, "Efficient, broadband and compact metal grating couplers for silicon-on-insulator waveguides," Opt. Express **15**, 9625-9630 (2007).
30. F. Liu, Q. Li, Z. Zhang, M. Qiu, and Y. Su, "Optically tunable delay line in silicon microring resonator based on thermal nonlinear effect," IEEE J. Sel. Top. Quantum Electron. **14**, 706-712 (2008).

1. Introduction

In recent years there has been an increasing interest aimed at the development of slow- and fast-light techniques, which can lead to a significant modification of the group velocity of a light pulse through a medium. Potential applications of slow-light and fast-light include controllable optical delay lines, optical buffers, true time delay for synthetic aperture radars, and cryptography and imaging in the quantum information field [1,2]. Fast light is challenging and interesting for the scientific community specifically in the context of information velocity [3-5], since superluminal signal velocities can be achieved without violating Einstein causality [6]. The fast light is typically achieved in a medium with a very large anomalous dispersion at the signal frequency. Experimental demonstrations of fast light have been realized based on stimulated Brillouin scattering (SBS) in optical fibers [7], coherent population oscillation in erbium-doped fiber amplifiers [8-10], alexandrite crystal [11] and quantum-dot semiconductor optical amplifiers (SOA) [12,13], four wave mixing processes in SOA [14], electromagnetically induced absorption in atomic vapors [5,15,16], negative refractive index property in a metamaterial [17], and structural dispersion in coupled resonator structures [18,19].

On the other side, the past several years have witnessed tremendous advancement in silicon photonics as silicon-on-insulator (SOI) structure provides an excellent platform for highly compact photonic devices and the processing technology is readily borrowed from the electronics industry [20,21]. The exploitation of resonances based on SOI structure to perform slow- and fast-light functions has been well received in terms of miniaturization and on-chip integration [22,23]. For the ring resonator, it has been commonly regarded that fast light can be only realized in the under-coupled region while over-coupling leads to slow light [18,19,24]. In this paper, we report experimental demonstration of fast light in over-coupled ultra-compact silicon ring resonator with resonance-splitting, relying on the large anomalous dispersion in the split resonances. By incurring a grating in the ring resonator, it induces mutual-coupling between the counter-clockwise travelling mode and the counter-propagating mode. In theory, we find that strong mutual-coupling can tune the effective phase shift from normal dispersion to anomalous dispersion for the over-coupled ring resonator, thus providing another approach to realizing fast light. For the under-coupled ring resonator, strong mutual-coupling can lead to resonance-splitting while the dispersion characteristic is preserved at resonance. In the experiment, a maximum pulse advancement of 130 ps with low distortion is

achieved for a 1-ns signal pulse in a 10-μm-radius silicon ring resonator, in good agreement with the theoretical results based on coupled mode theory. The mutual-coupling offers another degree of freedom when implementing resonance based slow- and fast-light functions.

2. Operational principle

We use the coupled mode theory to describe the operational principle. As illustrated in Ref [25], the resonance-splitting is caused by the mutual-coupling between the modes inside the ring resonator. The incident wave s_i only generates a counter-clockwise travelling mode a, which in turn induces b due to the grating that is present along the ring sidewalls, as shown in Fig. 1. The mode a and the mode b are related by the mutual-coupling coefficient u. k is the coupling coefficient between the ring and the bus waveguide. For the degenerate case, the mode a and b have the same resonance frequency ω_0, the decay rate due to loss $1/\tau_{int}$ and the decay rate into the bus $1/\tau_{cou}$. Near the resonant frequency, the evolution of the electric field a and b inside the resonator can thus be described by [25-27]:
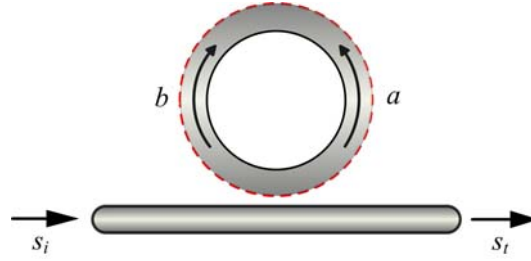

Fig. 1. Schematic illustration of a ring resonator side coupled to a waveguide with mutual-coupling. The grating is indicated as the red dashed circle.

$$\frac{d}{dt}a = \left(j\omega_0 - \frac{1}{\tau_{int}} - \frac{1}{\tau_{cou}} \right)a - jks_i - jub \tag{1}$$

$$\frac{d}{dt}b = \left(j\omega_0 - \frac{1}{\tau_{int}} - \frac{1}{\tau_{cou}} \right)b - jua \tag{2}$$

We define three quality factors: (1) intrinsic quality factor $Q_{int}=\omega_0\tau_{int}/2=\omega_0/(\alpha v_g)$, where α denotes the loss and v_g is the group velocity; (2) coupling quality factor $Q_{cou}=\omega_0\tau_{cou}/2=\omega_0/k^2$; (3) mutual-coupling quality factor $Q_{mut}=\omega_0/(2u)$ [25-27]. Given the equation connecting the incident field s_i and transmitted field s_t, $s_t=s_i-jka$, we obtain the transmission function of the ring resonator:

$$t = \frac{s_t}{s_i} = 1 - \frac{1}{2Q_{cou}}\left(\frac{1}{j\left(\delta + \frac{1}{2Q_{mut}}\right) + \frac{1}{2Q_{int}} + \frac{1}{2Q_{cou}}} + \frac{1}{j\left(\delta - \frac{1}{2Q_{mut}}\right) + \frac{1}{2Q_{int}} + \frac{1}{2Q_{cou}}} \right) \tag{3}$$

where $\delta=(\omega-\omega_0)/\omega_0$ denotes the normalized frequency detuning. For $Q_{mut}\rightarrow\infty$, Eq. (3) reduces to a single-ring without mutual-coupling case. We define a critical coupling parameter Q_{cri} $\left(1/Q_{cri}^2 = \left| 1/Q_{int}^2 - 1/Q_{cou}^2 \right| \right)$, which indicates the magnitude of the mutual-coupling needed to achieve resonance-splitting.

The effective phase shift Φ and the group delay τ can be denoted as $\Phi(\delta)=\arg(t)$ and $\tau=d\Phi(\delta)/d\delta$, respectively. The effective phase shift varies rapidly near resonator resonances and thus leads to strong normal or anomalous dispersion, corresponding to slow light or fast light, respectively. Both the transmission and dispersive behavior can be examined together on a parametric phasor plot of the transmission [28], which are shown in Fig. 2(a) for $Q_{cou}<Q_{int}$ and in Fig. 2(b) for $Q_{cou}>Q_{int}$, respectively. In the parametric phasor plot, the

modulus denotes the amplitude transmission while the phase angle denotes the effective phase shift. The black dots indicate $\delta=0$ and the green dots show $\delta=\pi$. The plots proceed counterclockwise as indicated around loop from $\delta=0$ to $\delta=2\pi$. For a value of δ, one can determine whether the signal is delayed or advanced simply by noting whether the effective phase shift is increasing or decreasing at the point of interest. Figure 3 depicts the normalized transmission, effective phase shift and group delay for $Q_{cou}<Q_{int}$ and $Q_{cou}>Q_{int}$, respectively.

For the over-coupling ($Q_{cou}<Q_{int}$) case, $Q_{mut}\rightarrow\infty$ corresponds to the case of an over-coupled ring resonator without mutual-coupling. Normal dispersion and correspondingly slow light can be achieved without mutual-coupling. As the mutual-coupling increases (Q_{mut} decreases from $+\infty$), the mutual-coupling enhances the resonance notch depth and has little impact on the effective phase shift and the delay if $Q_{mut}>Q_{cri}$. At $Q_{mut}=Q_{cri}$, the transmission is zero at resonance. However, once the mutual-coupling further increases ($Q_{mut}<Q_{cri}$), there exist two loops on the diagram and two minima are evident in the phasor plot, therefore resonance-splitting takes place. Figure 2(c) shows the zoom-in plot of the transmission phasor with resonance-splitting, in which $\delta=\delta^{(sp)}$ denotes the resonance-splitting points and $\delta=\delta^{(dr)}$ denotes the dispersion reversal points. At split resonances $\delta=\delta^{(sp)}$, anomalous dispersion and thus fast light takes place.

For the under-coupling ($Q_{cou}>Q_{int}$) case, the origin is always out of the loop. Therefore, the mutual-coupling lowers the resonance notch depth in the transmission and leads to anomalous dispersion if $Q_{mut}>Q_{cri}$. When $Q_{mut}<Q_{cri}$, resonance-splitting also takes place. Anomoulous dispersion and thus fast light can also be observed at the split resonances.
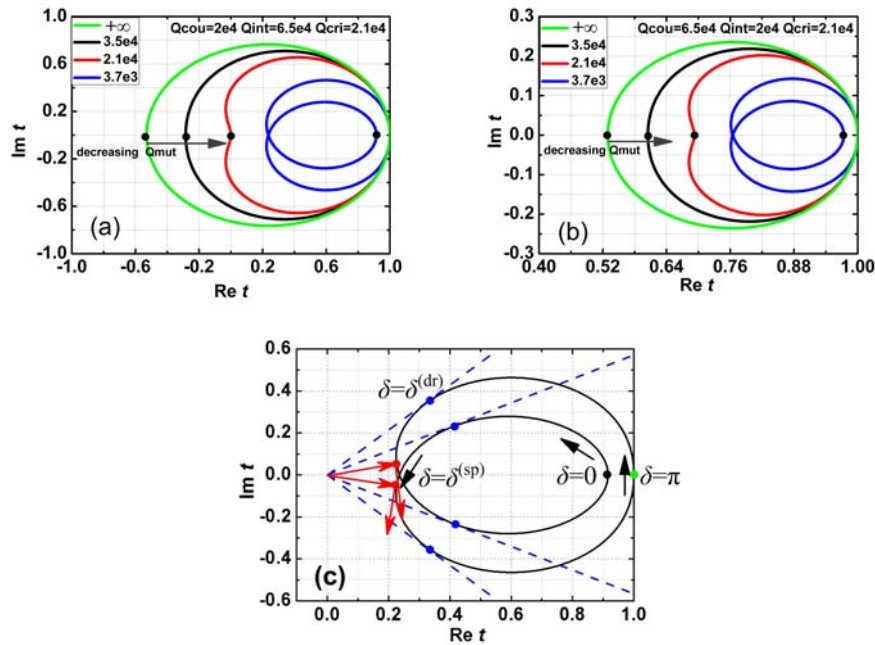

Fig. 2. Parametric phasor diagrams of the complex electric-field transmittivity for (a) $Q_{cou}<Q_{int}$ and (b) $Q_{cou}>Q_{int}$. The black dots indicate $\delta=0$ and the green dots indicate $\delta=\pi$. The plots proceed counterclockwise as indicated around loop (black arrows) from $\delta=0$ to $\delta=2\pi$. (c) is a zoom-in plot of the phasor diagram for $Q_{cou}<Q_{int}$ and $Q_{mut}<Q_{cri}$, showing that the transmission phasor and its gradient are perpendicular at split resonances, $\delta=\delta^{(sp)}$ (red dots) and that the transmission phasor and its gradient are parallel at points in which dispersion reversals occur, $\delta=\delta^{(dr)}$ (blue dots).
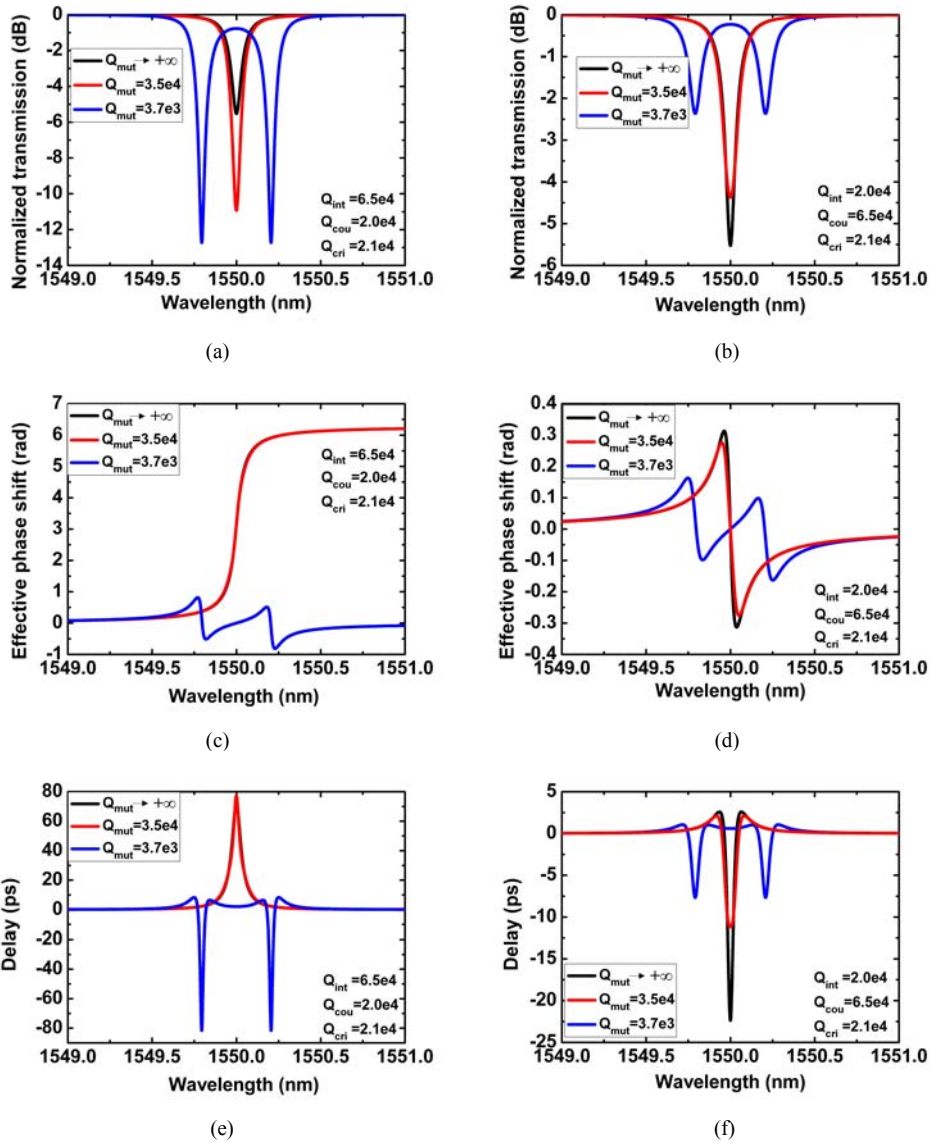
Fig. 3. Normalized transmission, effective phase shift and group delay for (a)(c)(e) $Q_{cou}<Q_{int}$ and (b)(d)(f) $Q_{cou}>Q_{int}$

Table 1 Dispersive responses of coupled resonators with mutual-coupling and the corresponding conditions.

Condition		Resonance-splitting	Dispersion response
$Q_{cou}<Q_{int}$	$Q_{mut}>Q_{cri}$	No	slow light
	$Q_{mut}<Q_{cri}$	Yes	fast light
$Q_{cou}>Q_{int}$	$Q_{mut}>Q_{cri}$	No	fast light
	$Q_{mut}<Q_{cri}$	Yes	fast light

*For $Q_{mut}=Q_{cri}$, the transmission on resonance is zero.

Table 1 summarizes the dispersive characteristics of coupled resonators with mutual-coupling, showing that resonance-splitting is always accompanied by fast light. For the over-coupled ring resonator, strong mutual-coupling can tune the effective phase shift from normal dispersion to anomalous dispersion; therefore fast light can be realized in the over-coupled ring resonator. For the under-coupled ring resonator, strong mutual-coupling can lead to resonance-splitting without reversing the dispersion characteristics at resonance.

3. Device characterization

The micro-ring resonator used in the experiments is fabricated on a commercial single-crystalline SOI wafer with a 250-nm-thick silicon slab on top of a 3-μm silica buffer layer. The radius of the ring is 10 μm. The ring/waveguide cross-section is 450×250 nm with an effective area of about 0.1 μm^2 for the transverse-electric (TE) mode. The microring is side coupled to the straight waveguide with an air gap of 120 nm. The waveguide and ring patterns are first defined in the E-beam lithography and transferred to the top silicon layer by reactive ion plasma etching. The waveguide is slowly tapered to a width of 10 μm at both ends, where gold gratings are added to couple light near-vertically from single mode fibers [29]. The grating couples only TE light with a minimal fiber-to-fiber loss below 20 dB. The scanning electron microscope (SEM) photo of the silicon microring resonator is provided in Fig. 4(a). Figure 4(b) shows the grating on the ring sidewall. The grating presents only in the microring. The width of the grating ridge is ~ 20 nm and the distances between adjacent grating ridges range from ~ 50 nm to ~ 100 nm. They are determined by a variety of parameters during the E-beam process, mainly the scan step size, line-scan intervals, exposure dose, and developing time, which has been detailed in Ref. [25]. By changing these parameters, the mutual coupling factor Q_{mut} and accordingly the splitting separation can be controlled during the fabrication.
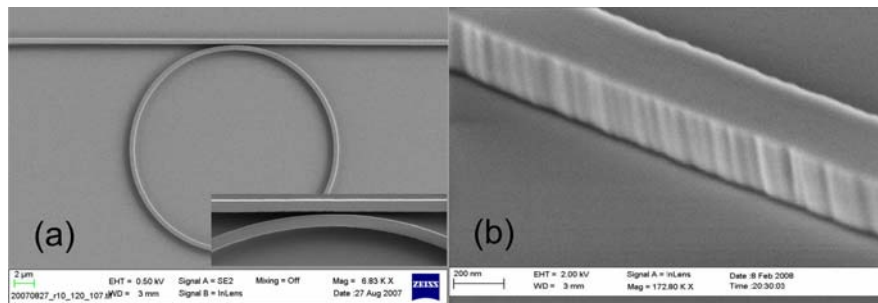

Fig. 4. SEM photos of (a) the silicon microring resonator with a radius of 10 μm and (b) the grating on the side-wall of the ring resonator. Inset in (a) is a zoom-in view of the coupling region

Figure 5 shows the spectral response of the ring resonator. The notches around 1550 nm are fitted using Eq. (1). For the 10-μm-radius ring resonator, the coupling Q_{cou}, intrinsic Q_{int}, and mutual-coupling Q_{mut} are 1×10^4, 1×10^5 and 1.5×10^3, respectively; while for the 5-μm-radius ring resonator they are 3×10^4, 4×10^4 and 1.37×10^4, respectively. The 10-μm-radius ring resonator has a stronger mutual-coupling and thus resonance-splitting is more obvious.
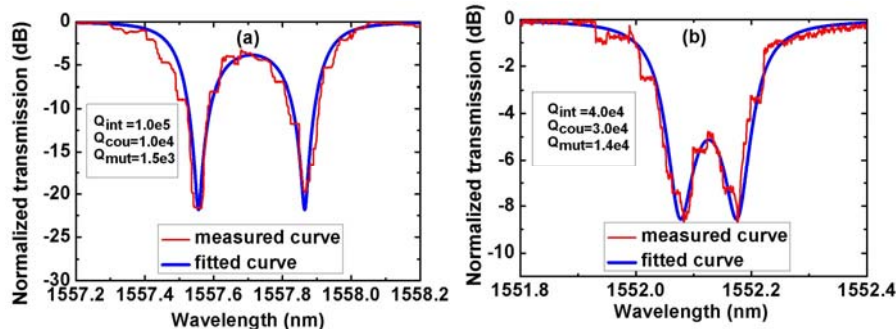
Fig. 5. The transmission spectrums with resonance-splitting for the (a) 10-μm-radius and (b) 5-μm-radius ring resonators. The red curves represent the measured transmission spectra and the blue curves are theoretical plots from the coupled mode equations.

4. Experiments and results

The schematic diagram of the experimental setup is depicted in Fig. 6. The signal source is a 500-Mb/s RZ pulse train with a duty cycle of 50% produced by two cascaded Mach-Zehnder modulators (MZMs). The full width at half maximum (FWHM) of the signal pulse is 1 ns. The generated signal is boosted by an erbium-doped fiber amplifier (EDFA) and then filtered by a tunable band-pass filter (BPF) with a bandwidth of 1.6 nm. The power sent into the input fiber is controlled below 0 dBm to avoid nonlinear effects. As the gold grating is polarization-sensitive, a polarization controller is inserted to make sure that the input probe lights are in TE mode. The output signal of the microring resonator is amplified by an EDFA and the noise is suppressed using another band-pass filter. An oscilloscope is used to record the temporal traces of the pulses after propagating through the ring resonator with resonance-splitting.
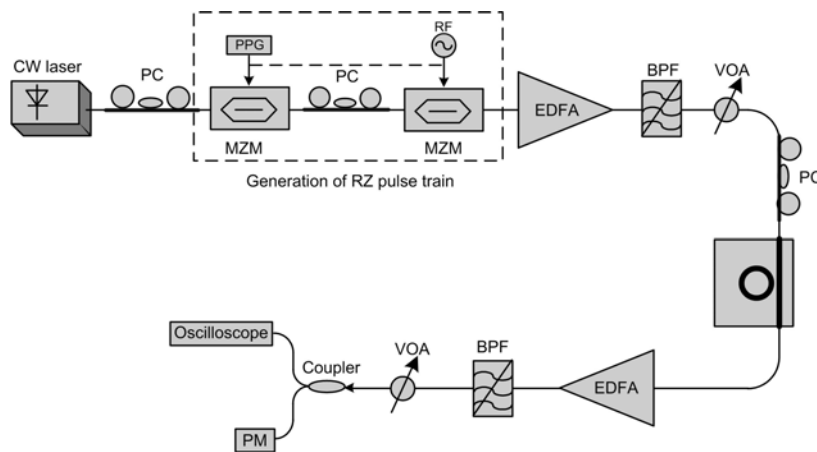

Fig. 6. Experimental setup. CW: continuous wave; PC: polarization controller; PPG: pulse pattern generator; MZM: Mach-Zehnder modulator; VOA: variable optical attenuator;

Figure 7 shows the normalized temporal signal waveforms after experiencing the fast light propagation through the ring resonator when the signal wavelength is on resonance. It is clearly observed that signal advancement is achieved with minor signal distortion. The achieved signal advancements are about 130 ps and 30 ps on resonance for the 10-μm-radius and 5-μm-radius ring resonators, respectively. Figure 8 shows the signal advancement as a function of signal wavelength, demonstrating that the advancement can be continuously tuned if the resonance of the microring can be varied [30]. The measured delays agree well with the theoretical calculation based on the coupled mode theory. Compared with the 4.9 ns advancement for a 65 ns signal that has been demonstrated in a fiber-based 56.5-μm-radius

ring resonator [19], our demonstration for the 10-µm-radius ring resonator has the advantages of a larger relative advancement and a more compact footprint.
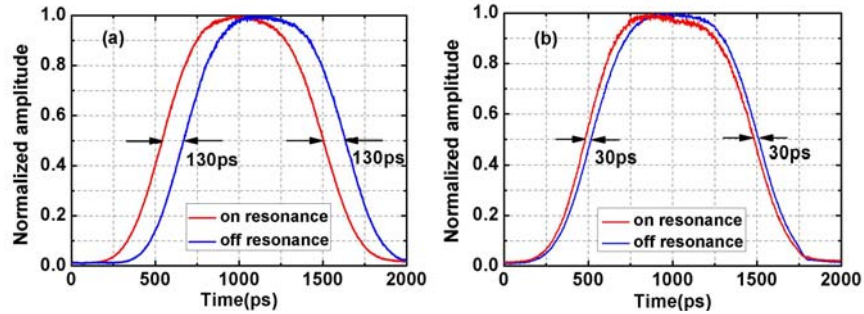

Fig. 7. The normalized traces of the pulsed signal showing clear advancements and minor signal distortion for the (a) 10-µm-radius and (b) 5-µm-radius ring resonators
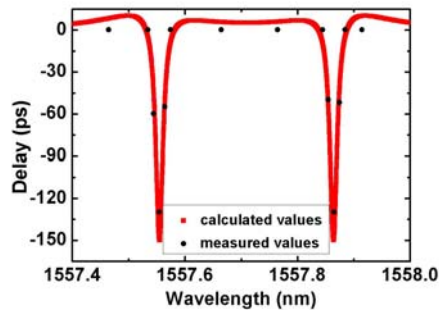

Fig. 8. Temporal advancements for 1-ns pulse signal with respect to the signal wavelength for the 10-µm-radius ring resonator

5. Conclusions

In this paper we report the experimental demonstration of fast light in the ultra-compact silicon ring resonator with resonance-splitting. For the over-coupled ring resonator, the induced strong mutual-coupling by the grating can tune the effective phase shift from normal dispersion to anomalous dispersion, thus fast light can be realized in the over-coupled ring resonator. In comparison, anomalous dispersion and fast light always exist despite the mutual-coupling for the under-coupled ring resonator. In the experiment, two ring resonators of 10-µm-radius and 5-µm-radius are fabricated, both operating in the over-coupling region ($Q_{cou}<Q_{int}$) and the 10-µm microring has a stronger mutual-coupling compared with the 5-µm one. For a 1-ns signal pulse propagating through the two ring resonators, the obtained maximum pulse advancements are 130 ps and 30 ps, respectively, agreeing well with the theoretical results based on the coupled mode theory. This demonstration in the resonance-split ring resonator provides a new approach to realizing fast light in an ultra-compact platform.

Acknowledgments